BIOCHEMISTRY
including biophysical chemistry & molecular biology

Article

pubs.acs.org/biochemistry

Development of a Reagentless Biosensor for Inorganic Phosphate, Applicable over a Wide Concentration Range

Claudia Solscheid,[†] Simone Kunzelmann,[†] Colin T. Davis,[†] Jackie L. Hunter,[‡] Annie Nofer,[‡] and Martin R. Webb*[,†]

[†]The Francis Crick Institute, Mill Hill Laboratory, The Ridgeway, Mill Hill, London NW7 1AA, United Kingdom
[‡]MRC National Institute for Medical Research, Mill Hill, London NW7 1AA, United Kingdom

ABSTRACT: A fluorescent reagentless biosensor for inorganic phosphate (P_i), based on the *E. coli* PstS phosphate binding protein, was redesigned to allow measurements of higher P_i concentrations and at low, substoichiometric concentrations of biosensor. This was achieved by weakening P_i binding of the previous biosensor, and different approaches are described that could enable this change in properties. The readout, providing response to the P_i concentration, is delivered by tetramethylrhodamine fluorescence. In addition to two cysteine mutations for rhodamine labeling at positions 17 and 197, the final variant had an I76G mutation in the hinge region between the two lobes that make up the protein. Upon P_i binding, the lobes rotate on this hinge and the mutation on the hinge lowers affinity ~200-fold, with a dissociation constant now in the tens to hundreds micromolar range, depending on solution conditions. The signal change on P_i binding was up to 9-fold, depending on pH. The suitability of the biosensor for steady-state ATPase assays was demonstrated with low biosensor usage and its advantage in ability to cope with P_i contamination.

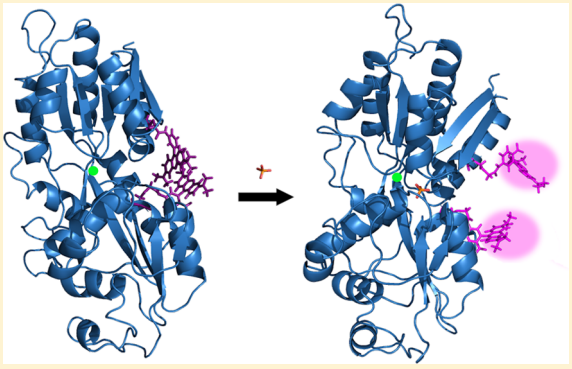

Inorganic phosphate (P_i) is a byproduct of numerous reactions in the cell, including metabolic reactions like fatty acid metabolism, energy transducing ATPases and cell signaling, such as by GTPases and protein phosphatases. Therefore, considerable effort has been expended to develop means of measuring P_i as a generic way to monitor such reactions. P_i assays, using complex formation with molybdate are widely used,[1−3] although they are not continuous. Several coupled enzyme assays have been described, particularly using a phosphorylase. Examples include the use of a fluorescent substrate, such as 7-methylguanosine[4] and one with an absorbance change, 2-amino-6-mercapto-7-methylpurine ribonucleoside,[5] or using other coupled enzymes to produce an absorbance or fluorescence change, for example with Amplex Red.[6] Fluorescent reagentless biosensors provide an alternative method of assaying P_i: they are single molecular species that respond to the particular analyte of interest with a change in fluorescence.[7] This approach circumvents some of the complexities of coupled enzyme assays, for example, in which multiple species are required as additives in the assay mix. Reagentless biosensors require a minimum of recognition element, such as a binding protein, and a reporter, here a fluorophore, in the same molecule, so no extra components are required for measurements.

The periplasmic phosphate binding protein (PstS) from *Escherichia coli*, here abbreviated to PBP, is a highly specific phosphate scavenger that has been used previously as the recognition element for fluorescent biosensors for P_i.[8,9] Fluorophores, covalently bound to surface cysteines, were the reporters for P_i binding, responsive to P_i concentration in the medium. A diethylaminocoumarin-labeled version of the protein (MDCC-PBP) typically has a 7-fold signal change,[8] whereas a tetramethylrhodamine-labeled biosensor (rho-PBP) results in up to an 18-fold signal increase.[9] Both of these biosensors bind P_i at rates suggesting diffusion control and with dissociation constants in the nanomolar range. These have been particularly useful to measure P_i production or release in real time in a wide range of enzymatic systems in vitro, particularly in transient kinetic assays,[10−14] but have also been developed into other formats, such as attachment to an optical fiber.[15]

While this fast response and the tight binding of the original PBP-based biosensors enables the study of reactions that release P_i rapidly, these same properties also necessitate the sensor to be present at an excess over P_i, as essentially all P_i binds to the protein in almost all assay conditions. The biosensors typically measure P_i in tens of nanomolar to low micromolar range. The tight binding also renders them sensitive to even low levels of P_i contamination, which can be present in solutions or on surfaces and particularly occurs with such molecules as nucleotides.[16,17] The relatively high consumption of stoichiometric biosensors may also be a

Received: April 24, 2015
Revised: July 22, 2015
Published: July 22, 2015

DOI: 10.1021/acs.biochem.5b00449
Biochemistry 2015, 54, 5054−5062

limiting factor for high-throughput assays and P_i contamination may require extra precautions or purifications of reagents used.

It is, therefore, desirable to have biosensors with different properties to expand the range of applications and types of assay. In particular, a variant of rho-PBP is described here with much lower affinity for P_i, but retaining a fluorescence change on P_i binding. This means that the biosensor can be used substoichiometrically relative to the P_i and that it can tolerate significant P_i contamination. In addition a biosensor with a lower affinity can be used for assays where higher micromolar amounts of P_i are released. This is a potential advantage in high-throughput and steady-state assays that are typically carried out over time scales of minutes.

Like the other members of the periplasmic binding protein superfamily, the phosphate binding protein is formed of two lobes linked by a hinge region and the P_i binding site is located in the cleft between these lobes.[18] The protein undergoes a large conformational change upon ligand binding including a bending motion of the two lobes around the hinge.[19] To produce the biosensor, fluorophores were attached to cysteines introduced on the surface so that their environment changes when this P_i-induced conformation change occurs.[9,20] In MDCC-PBP, a single diethylaminocoumarin was attached to one lobe at the top of the cleft and its interaction with the protein changes upon the conformation change. In rho-PBP, a tetramethylrhodamine (TMR) was attached on either side of the cleft such that in the apo form the rhodamine rings can stack, exhibiting very low fluorescence.[21] The P_i-induced conformation change causes partial disruption of the stacking interaction and the fluorescence increases.[9]

When introducing further mutations to weaken binding, it was important not to lose the fluorescence signal on P_i binding. In the rho-PBP construct, the main interactions of the rhodamines are with each other and not the protein, potentially making its fluorescence response less susceptible to changes to the protein. Because of this, together with its large fluorescence response and the high photostability of rhodamines, rho-PBP was chosen as the starting point to develop a weak-binding variant. As part of this development, several different strategies were explored to investigate where which parts of the PBP structure might be altered by mutation. Two approaches were to disrupt either the binding of the phosphate itself or the associated conformational change, namely cleft closure. A third approach was to mutate the hinge between the lobes. Protein variants of each type are described with their relative success. The final biosensor carries the I76G mutation in the hinge in addition to the A17C and A197C previously introduced for labeling with TMR.[9] Properties of this variant, including its interaction with P_i, phosphate analogues and nucleotides are described. Its useful range is characterized and an example assay to measure P_i production rate is shown.

EXPERIMENTAL PROCEDURES

Materials. "Bacterial" purine nucleoside phosphorylase was obtained from Sigma and dissolved to 1000 U mL^{-1}. PcrA helicase was purified as described.[22,23] Oligonucleotide dT_{35} and nucleotides were from Sigma. 6-Iodoacetamidotetramethylrhodamine (6-IATR) was a gift from Dr. J. Corrie (NIMR, London).[24,25]

Expression and Purification of Phosphate Binding Protein. PBP mutants were created in pET22b harboring the gene for mature *E. coli* (A17C,A197C)PBP between Nde1 and Xho1 sites in the MCS using a Quikchange site-directed mutagenesis kit (Stratagene) according to manufacturer's instructions. A stop codon was inserted at the end of the *Pst*S ORF, so that the encoded His_6-tag was not added to the polypeptide chain. Plasmids were sequenced (GATC Biotech) to confirm the presence of the desired mutation(s). Previously PBP was expressed from the full gene, induced by P_i starvation, and so included the N-terminal signal peptide that was lost in the mature protein.[9,26] The pET22 vector described above produced a protein identical to the mature PBP except for an additional N-terminal methionine. It has an advantage of simple induction by IPTG. The amount of purified (A17C,A197C)-PBP from this new construct was comparable to the previous method and typically 300 mg from 4 L of *E. coli* culture. An equivalent construct produced similar amounts of (A197C)PBP for MDCC labeling. Note that amino acid numbering is based on the natural, mature wild-type protein.

Plasmid pET22b carrying the desired mutations within the *Pst*S ORF encoding PBP was transformed into BL21 (DE3) and used for preparing rho-PBP variants. An overnight culture was grown in LB medium containing 100 μg mL^{-1} ampicillin at 37 °C with aeration by vigorous shaking. This culture was diluted 50-fold into 500 mL aliquots of fresh medium and grown to an $OD_{600} \sim 0.8$ before expression was induced with 500 μM IPTG. After 4 h induction, cells were harvested by 20 min centrifugation at 2500*g* and 4 °C. Cells were resuspended in 20 mM Tris-HCl pH 8.0 and stored at −80 °C.

For purification, cells from 500 mL culture were thawed and sonicated 4 × 30 s at 200 W with a 5 s on/off pulse cycle. The lysate was cleared by centrifugation at 142 000*g* and 4 °C for 45 min. A 5 mL HiTrapQ FF column (GE Healthcare) was equilibrated in 10 mM Tris-HCl pH 8.0, 1 mM dithiothreitol (DTT). The conductivity of the supernatant was adjusted to that of the buffer before applying it to the column. Protein was eluted in a 50 mL gradient of 0−200 mM NaCl in 10 mM Tris-HCl pH 8.0. Fractions containing PBP were pooled and concentrated in a Vivaspin 20 concentrator (MWCO 10 kDa, GE Healthcare), yielding ∼130 mg of PBP per liter culture.

To determine the quarternary structure of (A17C, I76G, A197C)PBP it was applied to a Superdex 200pg 16/60 size exclusion column equilibrated in 10 mM Tris-HCl pH 8, 150 mM NaCl, 1 mM NaN_3. The protein ran as single species corresponding to the size of the monomer.

Labeling. Purified PBP was labeled with 6-IATR as described previously[9] in 10 mM Tris-HCl pH 8.0, 100 mM NaCl. The mixture was then slowly diluted to ∼3 mM NaCl and concentrated prior to separation of free label and labeled protein. Precipitate was removed from the soluble protein fraction by centrifugation at 16 000g for 10 min at 4 °C, and the supernatant filtered through a 0.2 μM polysulfone membrane (PALL Life Sciences). The protein was then applied to a 1 mL MonoQ HR 5/5 column (GE Healthcare) equilibrated in 10 mM Tris-HCl pH 8.0. The protein was eluted with a 30 mL gradient of 0−100 mM NaCl. The elution profile showed three peaks, with the major, second peak eluting at around 20 mM NaCl.

As determined by mass spectrometry and the ratio of absorbance of label (526 nm) and protein (280 nm), this fraction corresponds to the double-labeled PBP. It was concentrated and further analyzed as described below. The variant used for further study was (A17C,I76G,A197C)PBP, labeled with 6-IATR and this is termed rho-PBPw. The concentration of rho-PBP was calculated using an extinction coefficient of 108 mM^{-1} cm^{-1} at 526 nm.[9]

DOI: 10.1021/acs.biochem.5b00449
Biochemistry 2015, 54, 5054−5062

Absorbance and Fluorescence Measurements. Absorbance spectra were obtained on a JASCO V-550 UV/vis spectrophotometer. Fluorescence spectra and titrations were obtained on a Cary Eclipse fluorimeter with xenon lamp. Stopped-flow experiments were performed using a HiTech SF61MX apparatus with mercury−xenon lamp and HiTech Kinetic Studio software (TgK Ltd., U.K.). There was a monochromator and 4 mm slits on the excitation light (548 nm) and a 570 nm cutoff filter on the emission. The concentrations given are those in the mixing chamber unless otherwise stated, and data were fitted to theoretical curves using HiTech software and Grafit 7.[27]

Circular Dichroism. Near- and far-UV spectra were recorded in 1 mm fused silica cuvettes using a JASCO J-815 spectropolarimeter at 20 °C.

Steady-State ATPase Rate Measurements. Rho-PBPw was used to measure the steady-state ATP hydrolysis of the DNA helicase PcrA. Measurements were carried out in 50 mM Tris-HCl pH 7.5, 150 mM NaCl, 3 mM $MgCl_2$ containing 4 nM PcrA, 100 μM ATP, 5 μM BSA, 3 μM rho-PBPw, and dT_{35} at concentrations ranging from 25 to 300 nM. Reactions were followed using the fluorescence detection setting on a CLARIOstar Microplate Reader (BMG Labtech) with excitation at 546 nm and emission at 580 nm.

RESULTS

Design Approach. In order to extend the useful range of the existing rhodamine-labeled phosphate biosensor[9] to a wider concentration range, the affinity of PBP for P_i had to be lowered by mutation. This could, in principle, be accomplished by several means, given that the two lobes are largely unchanged internally by P_i binding: only their relative position and orientation changes as they enclose the bound P_i. Most obviously and directly amino acids associated with P_i binding could be changed, disrupting binding interactions. Second, the associated conformational change could be targeted by modifying amino acids that are in the cleft and modify its closure, but are not involved in P_i binding. Third, the conformation change, and therefore P_i binding, might be affected by modifying the flexibility of the hinge between the two lobes. Several mutation sites in these three areas were identified, based on crystal structures[18,19,28] (Figure 1 and Table 1) and each approach is described in turn. Each PBP variant was labeled on the two cysteines by 6-iodoacetaminotetramethylrhodamine (6-IATR): the fluorescence of this product was used to assess the response to P_i.

Binding-Site Mutations. The crystal structures of PBP, bound with P_i, show a large number of potential hydrogen bonds between amino acids and the four oxygen atoms of P_i.[18] Previously PBP with the binding site mutation T141D was used to obtain the crystal structure of the apo protein, as this was shown to have weakened, but highly pH-dependent, binding of P_i.[19] A study of the phosphate binding protein from the cyanobacterium *Synechococcus* sp. identified several active site residues affecting phosphate affinity.[29] Although sharing only 37% sequence identity, it was predicted to have high structural homology with the *E. coli* protein, with all but one active site residue between the species being conserved. In *Synechococcus* sp., replacement of active-site residues lowered phosphate affinity by up to 5 orders of magnitude.

Based on observation of the crystal structures and these data, single or double mutations were introduced into the *E. coli* PBP as listed in Table 1 and shown in Figure 1C. With ∼1000-fold

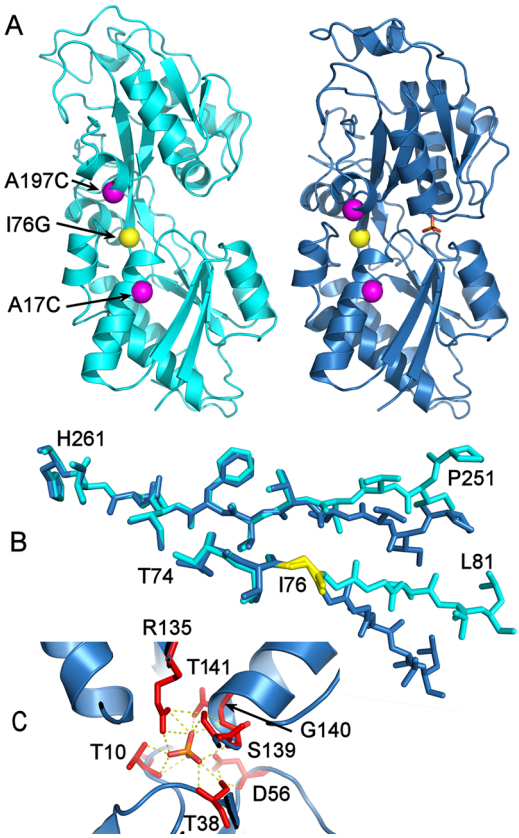

Figure 1. Structure of *E. coli* phosphate binding protein, highlighting active site residues and mutations tested. (A) Complete structure, indicating residues altered in rho-PBPw. Apo PBP is cyan and P_i-bound PBP dark blue.[18,19] The mutation site in the hinge region (I76G) is in yellow, the sites for rhodamine attachment (A17C, A197C) are in magenta. (B) The hinge region from the same structures, showing the movement between apo (cyan) and P_i-bound PBP (dark blue). I76 is shown in yellow. (C) Binding site residues modified are shown as red sticks, and putative bonds between residues and P_i are shown as yellow dashed lines.

decrease compared to the original tight-binding PBP sensor, S38A (K_d 68 μM) and G140A (70 μM) showed the largest change in P_i affinity. Residue R135, forming contacts with two of the phosphate's oxygens and other residues close to the active site,[18] was also mutated. While this R135A variant showed the largest fluorescence change between apo and P_i-bound PBP, binding remained tight. The T141D variant of MDCC-PBP was also tested, but both the fluorescence change and affinity were highly dependent on pH, as shown previously, with the K_d changing by ∼3 orders of magnitude between pH6.0 and 8.5[11,19] and so was not included in this survey. This would make application of that variant as a biosensor difficult. In addition, some pairs of mutations were also tested in combination, but failed to give a significant fluorescence response, and so their phosphate affinity could not easily be determined. Overall for these variants with binding site mutations, large changes in affinity were accompanied by considerable loss of fluorescence change on P_i binding.

Cleft Mutations. The second approach was based on targeting the cleft closure by affecting the interactions between the facing, inner surfaces of the two lobes.[30−32] This might be achieved by changing amino acids that have interactions across the closed cleft with residues on the opposite side or by changing residue size. Several residues on the lobe surfaces

DOI: 10.1021/acs.biochem.5b00449
Biochemistry 2015, 54, 5054−5062

Table 1. Survey of Mutations to Weaken Binding[a]

label sites	mutations	location	fluorescence ratio ($+P_i/-P_i$)	K_d [μM]
A17C, A197C		N/A	18	0.07[b]
	T10A	active site	2.2	32 ± 2
	S38A	active site	1.5	68 ± 9
	R135A	active site	4.5	tight[c]
	G140A	active site	2.8	70 ± 17
	T10A, G140A	active site	<1.1	ND
	S139A, T141A	active site	<1.2	ND
	I76G	hinge	5.9	7.4 ± 0.4
	K200A	cleft	2.1	ND
	G140A, A225Q	cleft	<1.1	ND
	G140A, A225Y	cleft	1.0	ND
	S39D, S164 K, G140A	cleft	1.0	40 ± 4
K229C, E302C	T10A	active site	1.2	ND
	G140A	active site	2.5	220 ± 11

[a]Amino acids are numbered based on the sequence of the mature PBP. Cysteine mutations for fluorophore attachment are indicated as "label sites", while "mutations" denote residues altered to lower P_i affinity. The location denotes the general area of the protein where the mutation was introduced. The fluorescence change is the ratio between the signal at saturating P_i concentrations to that containing P_i mop. For variants showing a significant fluorescence change, the P_i affinity was determined by titration of 1 μM rho-PBP variant with P_i in 10 mM Pipes pH 7.0. The maximum signal change and the K_d value were determined typically from three independent titrations. [b]Values for the "parent", tight-binding protein are taken from Okoh et al., where the K_d was calculated from the ratio of rate constants.[9] [c]This protein showed tight-binding, with dissociation constant ~1 μM or lower.

were mutated (Table 1). In all cases the P_i-dependent fluorescence change was almost completely lost and so the affinities of these variants for P_i were not determined.

Hinge Mutations. The final approach, in which the flexibility of the hinge region was altered, proved most successful. The hinge consists of two peptides, approximately parallel and linking the two lobes. Cleft closure is achieved by a bending rotation of the hinge (Figure 1B). A double glycine in the sequence provides flexibility and to increase this, a neighboring isoleucine was replaced with a further glycine resulting in a triple glycine stretch. This residue is located at the point of flexion associated with the rotational movement during the conformational change. The I76G variant of the TMR-labeled (A17C, A197C)PBP responded to P_i with a large fluorescence change and showed the desired reduction in affinity. The combination of these characteristics made this variant, from here on described as rho-PBPw, the best candidate for further characterization.

Spectral Properties of rho-PBPw. On binding P_i to rho-PBPw, the absorbance spectrum of the rhodamine changed (Figure 2), with the peak at 515 nm decreasing and the peak at 555 nm increasing. This is typical of two rhodamines shifting from a stacked configuration toward unstacked[33] and is similar to that observed in the original tight-binding rho-PBP.[9] The isosbestic point was 526 nm (Figure 2 inset).

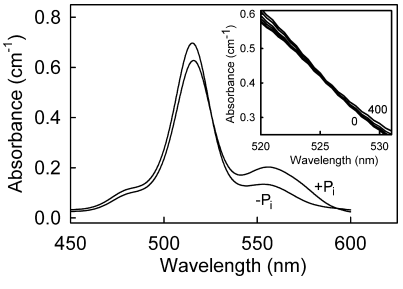

Figure 2. Absorbance spectra of rho-PBPw. Spectra of 1 μM rho-PBPw with 200 μM P_i or phosphate mop (0.1 U mL^{-1} purine nucleoside phosphorylase, 200 μM 7-methylguanosine) ($-P_i$) in 10 mM Pipes pH 7.0, 100 mM NaCl. Inset: Traces with 0–400 μM P_i, showing that the isosbestic point was 526 nm.

The fluorescence spectra showed a maximum increase of around 9-fold on binding P_i (Figure 3), with excitation and emission maxima of 556 and 577 nm, respectively. This fluorescence change was used to measure P_i affinity, by titrating P_i into the apoprotein, giving a dissociation constant (K_d) of 28 μM (Figure 4).

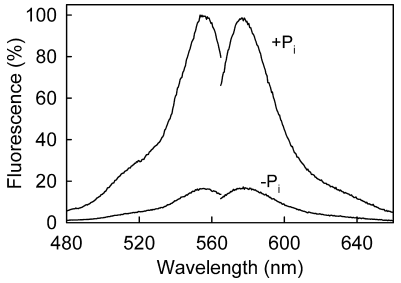

Figure 3. Fluorescence spectra of rho-PBPw. Spectra of 1 μM rho-PBPw with either 200 μM P_i ($+P_i$) or phosphate mop (0.1 U mL^{-1} purine nucleoside phosphorylase, 200 μM 7-methylguanosine) ($-P_i$) were obtained in 20 mM Pipes pH 7.0, 100 mM NaCl. Excitation spectra were measured by emission at 577 nm. Emission spectra were obtained by excitation at 555 nm.

To confirm that there were no gross changes to secondary structure by this additional mutation, far UV circular dichroism spectra were obtained (data not shown). Both rho-PBP and rho-PBPw had spectra identical to each other and unchanged in the 200–250 nm region in the presence and absence of saturating P_i. These spectra were also identical to those reported for MDCC-PBP.[20]

Variation of Fluorescence Response with Solution Conditions. Both the affinity of rho-PBPw for P_i and the fluorescence change on binding P_i varied with pH and salt concentration (Table 2). The main features are that the amplitude of the signal change decreased with increasing pH,

DOI: 10.1021/acs.biochem.5b00449
Biochemistry 2015, 54, 5054–5062

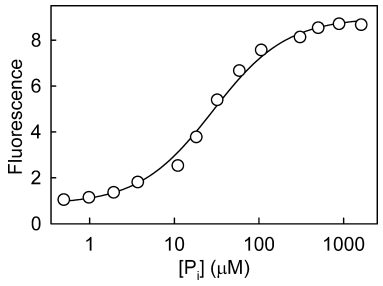

Figure 4. Titration of rho-PBPw with P_i. Two μM rho-PBPw were titrated against P_i at 20 °C in 20 mM Pipes pH 7.0, 100 mM NaCl, and 5 μM BSA. Aliquots of P_i, adjusted to pH 7.0, were added, and fluorescence intensity corrected for the dilution. Data were fitted to a quadratic binding curve[38] with a K_d of 28 ± 3 μM and an 8.7-fold fluorescence change.

Table 2. Fluorescence Change and Affinity at Different pH Values and Salt Concentrations[a]

pH	NaCl [mM]	fluorescence ratio (+P_i/−P_i)	K_d [μM]
6.5	20	6.4 ± 1.1	11 ± 2
	150	8.9 ± 1.4	39 ± 5
7.0	0	5.0 ± 0.3	4.2 ± 0.4
	20	5.5 ± 0.4	15 ± 1
	150	7.2 ± 0.8	50 ± 8
7.5	20	4.4 ± 0.9	25 ± 4
	150	5.4 ± 0.4	121 ± 16
8.0	20	2.1 ± 0.1	39 ± 9
	150	2.6 ± 0.2	120 ± 28
8.5	20	1.8 ± 0.1	33 ± 3
	150	2.0 ± 0.1	103 ± 20

[a]Fluorescence titrations were obtained as described in Figure 4. Measurements at pH 6.5 and 7 were in 20 mM Pipes, and those at pH 7.5−8.5 in 50 mM Tris-HCl. The fluorescence ratio is between the signal at saturating P_i concentrations to that of the solution prior to P_i addition. The value displayed corresponds to the signal change obtained from the fit to the titrations as in Figure 4, rather than from spectra. Measurements were done on at least three experimental replicates and two separate protein preparations, which were then combined for fitting.

but did not change significantly with salt concentration. The dissociation constant did not vary much with pH at low salt (8.3 μM at pH 6.5 to 46 μM at pH 8.5), but increased more at high salt. There was also a several-fold increase with salt concentration. The maximum signal change was ∼9-fold in 20 mM Pipes pH 6.5, 150 mM NaCl.

Limit of P_i Binding Kinetics. With the tight-binding variants, rho-PBP and MDCC-PBP, P_i binding was interpreted as occurring in a two-step mechanism, namely, diffusion-controlled binding to the open conformation of PBP, followed by the cleft-closing conformation change.[9,20] It is the latter that produces the fluorescence change. It is likely that the reduced affinity of rho-PBPw is accompanied by a combination of slower binding and/or faster dissociation. To test this, the time course was measured, following rapid mixing of rho-PBPw with P_i, using fluorescence stopped-flow. At all the concentrations of P_i tested, no fluorescence change occurred during the observed time course, which starts after the dead time of the stopped-flow instrument (2 ms). However, the fluorescence intensity, although constant with time, increased with P_i concentration with a similar dependence as the steady-state titrations (Figure 5). This suggests that the transient fluorescence change on binding was complete within the dead time and only the final, P_i-bound fluorescence was observable.

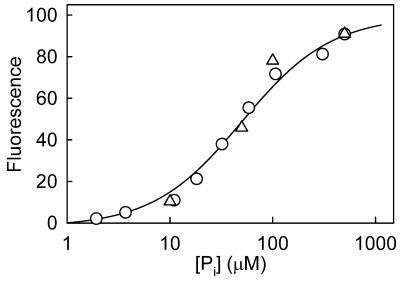

Figure 5. Comparison of fluorescence intensities of rho-PBPw, following stopped-flow mixing with P_i and end-point titration. P_i at various concentrations was mixed with 1 μM rho-PBPw in 20 mM Tris-HCl pH 7.5, 150 mM NaCl and 5 μM BSA at 20 °C in a stopped-flow apparatus. No change in fluorescence was observed during the time courses, suggesting the reaction was complete within the dead time of the instrument (2 ms). However, the constant intensity for each trace increased with [P_i]. As a control and to get the background fluorescence, 1 μM rho-PBPw was mixed with buffer. To confirm that the fluorescence intensities were those of the final P_i-bound form, an end-point titration was done in a cuvette under exactly the same solution conditions and the fluorescence changes (circles) compared with the stopped-flow data (triangles). To enable the comparison of data obtained using the different optics, the fluorescence intensities were adjusted to have the same values at 500 μM P_i. The combined data were fitted to a quadratic binding curve (K_d of 50 ± 8 μM).

To provide further evidence for this interpretation, an attempt was made to measure the dissociation kinetics directly by rapidly mixing rho-PBPw·P_i with a large excess of unlabeled, but high affinity PBP, as previously done to measure the dissociation kinetics of high affinity rho-PBP.[9] In this case, no fluorescence change was observed (data not shown), suggesting that dissociation was rapid and complete within the dead time.

Specificity. Wild-type PBP and the original phosphate biosensors showed high selectivity for inorganic phosphate.[9,18] In order to establish whether lowering the affinity had a significant effect on specificity, rho-PBPw was titrated with a selection of P_i analogues, pyrophosphate, and nucleotides (Table 3). No significant fluorescence response was obtained from addition of the main competing ligands. The P_i analogues chosen were those that did give a response with the tight-binding P_i sensor, namely, arsenate and vanadate: neither gave a response at the concentrations tested.

Comparison of Fluorescence Intensity Levels of TMR. The rhodamine fluorescence intensity of rho-PBPw was compared with the tight-binding variant and tetramethylrhodamine in solution. The fluorescence quantum yield is difficult to measure accurately when the emission spectrum extends to high wavelength, where corrections are large. To circumvent this, a simpler measure was used by dividing the corrected fluorescence emission intensity at the maximum wavelength by the absorbance at the excitation maximum. This ratio was then used to give an approximate comparison between different species containing the same tetramethylrhodamine fluorophore (Table 4). This shows that the rhodamine is much less fluorescent when attached to the (A17C, I76G, A197C)PBP than in free solution or attached to a small molecule thiol, but does not change greatly on P_i binding.

Steady-State Assay of P_i Production. To test rho-PBPw, the ATPase activity of PcrA, a DNA helicase, was measured in a

DOI: 10.1021/acs.biochem.5b00449
Biochemistry 2015, 54, 5054−5062

Table 3. Response of rho-PBPw to P_i Analogues and to Nucleotides[a]

species	fluorescence ratio ($+P_i/-P_i$)
ATP[b]	1.1
ADP[b]	1.1
GDP[b]	1.5
PP_i[b]	0.9
sodium arsenate	1.1
sodium vanadate	1.0

[a]The species tested were added to 5 μM rho-PBPw in 20 mM Pipes pH 7.0, 100 mM NaCl. Fluorescence emission spectra of the solution $\pm$100 μM of the respective species were measured as described for Figure 4. Saturating P_i was subsequently added to each mixture to verify sensor response. The fluorescence ratio was calculated from the baseline fluorescence of the solution prior to substrate addition and the resultant fluorescence after addition. The highest signal change was observed for GDP, but may be explained by contaminating P_i in the nucleotide stocks. [b]These were treated with phosphate mop (1 U ml^{-1} purine nucleoside phosphorylase, 200 μM 7-methylguanosine)[16] for 15 min at room temperature to reduce contaminating P_i, prior to addition to rho-PBPw. The phosphorylase activity may be inhibited by the presence of purine nucleotides at high concentration, limiting the effectiveness of this treatment.

Table 4. Relative Fluorescence Intensities of Tetramethylrhodamines[a]

species	relative fluorescence
6-IATR in EtOH	1
6-IATR in buffer	0.42
6-IATR-MESNA	0.51
rho-PBPw, P_i	0.08
rho-PBPw, no P_i[b]	0.03
rho-PBP, P_i	0.13
rho-PBP, no P_i[b]	0.07

[a]Apart from the 6-IATR sample in ethanol, all measurements were in 10 mM Pipes pH 7.0, 100 mM NaCl using solutions with a maximal absorbance of <0.05. The fluorescence spectra were then corrected for the photomultiplier profile and baseline. The fluorescence intensity at maximum emission was divided by the absorbance at maximum excitation. The relative fluorescence was normalized to that of 6-IATR in ethanol. [b]Solutions were treated with phosphate mop as described in Figure 3.

multiwell plate format (Figure 6). PcrA couples ATP hydrolysis to translocation along single-stranded DNA, using one ATP molecule per translocation step of one base.[34] This ATPase activity has been well characterized using the high-affinity phosphate sensor under identical solution conditions[35] and so provided a good test of the new biosensor. Both the K_m (88 nM) for dT_{35} and k_{cat} (32 s^{-1}) obtained using rho-PBPw are similar to the previous measurements. Using the new biosensor a larger range of P_i could be monitored (up to 80 μM). In addition, the lowered affinity rendered the sensor less sensitive to contaminating P_i, so that no phosphate mop was required to remove such contaminant.[16]

DISCUSSION

The affinity of the original P_i biosensor, rho-PBP,[9] was altered by inserting mutations in strategic positions of the PBP scaffold. Kinetic and other measurements on the fluorescent, tight-binding PBP suggested a rapid, possibly diffusion controlled initial binding of P_i to the open conformation, followed by a rate-limiting cleft closure.[9,20] In principle, the affinity could be

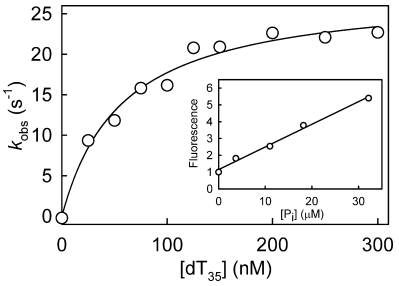

Figure 6. Steady-state ATPase activity of PcrA. Measurements were carried out at 18 °C in 20 mM Tris-HCl pH 7.5, 150 mM NaCl and 3 mM $MgCl_2$. Reactions contained 4 nM PcrA, 3 μM rho-PBPw, 100 μM ATP, and dT_{35} at various concentrations. The concentration dependence of initial rates was fitted to the Michaelis–Menten equation to give a K_m for dT_{35} of 88 $\pm$ 13 nM and a k_{cat} of 32 $\pm$ 1 s^{-1}. The Inset shows a calibration under the same conditions.

altered by changing either step of this mechanism. Three parts of the structure were targeted for mutations that might affect the binding, namely the binding site, interlobe cleft surfaces and the hinge region between the two lobes.

The P_i-binding site is highly specific, being able to discriminate against similar molecules such as sulfate. It contains 12 residues that form hydrogen bonds with the four oxygens of the P_i.[18] While most of these residues are hydrogen donors, D56 is a hydrogen bond acceptor and plays a crucial role in substrate recognition and discrimination. On the whole for binding site mutations, a large reduction in affinity was accompanied by a large reduction in the signal change on binding P_i. This meant that mutations in the binding site did not give a suitable candidate weak-binding variant. Moreover, there were significant differences in effects of mutations in the *E. coli* protein, used here, from those described for *Synechococcus* PBP, predicted to be a close structural homologue.[29] For example, the T10A mutation, which resulted in a large loss of affinity (5 orders of magnitude) in the *Synechococcus* PBP, whereas there was a much smaller change in affinity, ~ 500-fold lower, in the *E. coli* protein. The difference in effect of active site mutations cannot, therefore, be exclusively due to changes in the active site residues, as these are conserved between the two species, even though overall the proteins share only moderate sequence homology. Active site mutations may have varied secondary effects on the two proteins, due to differences in their amino acid composition. In addition, different signal elements were used in the two biosensors, a small fluorophore here and fluorescent protein with the *Synechococcus* PBP. This, as well as the different sources of the two PBPs, may provide an explanation of the differences observed.

Mutations to the cleft surface resulted in small or no signal change upon P_i addition, so the affinity could not be readily determined. Although the predicted structure of the rhodamines in the apo structure suggests little contact with surface amino acids,[21] this aspect is little understood and mutations in the cleft might affect indirectly the structural changes that disrupt the rhodamine interaction. In other words, mutations that weaken the interaction across the cleft may mean that cleft closure becomes unfavored thermodynamically. Measurements with the tight-binding variant, rho-PBP, suggest that the cleft closing conformation change on rho-PBP·P_i occurs subsequent to P_i binding itself and has an equilibrium constant of 40 in

DOI: 10.1021/acs.biochem.5b00449
Biochemistry 2015, 54, 5054–5062

favor of closure,[20] so only a small change in this equilibrium constant will be significant in this respect.

The most successful strategy for lowering P_i affinity, while maintaining a fluorescence signal, was altering the hinge between two lobes making up PBP. Insertion of a third glycine residue at position 76 in the hinge (Figure 1B) lowered P_i affinity up to several hundred-fold, compared to the tight-binding sensor, but maintained a reasonably large signal change (Table 1). This extra mutation is on the opposite side of the protein from the rhodamines (Figure 1A), so may be unlikely to affect their fluorescence directly. The fact that the replacement amino acid is glycine suggests the possibility that the hinge is now more flexible. Circular dichroism measurements show no significant changes to secondary structure due to this mutation.

Presumably the cleft-closing conformation change is still favored thermodynamically in rho-PBPw, in order to result in net cleft closure and produce the fluorescence change. So the main effect of I76G would be on the equilibrium constant of the binding step itself, either slowing binding or increasing dissociation rate constants.

Stopped-flow kinetic measurements were unable to give precise kinetic information as the binding and dissociation kinetics were too fast to measure. However, the data suggested that the sum of rate constants for dissociation must be >1800 s^{-1} for the reactions to be almost complete within the 2 ms dead time of the stopped-flow instrument, even at low P_i concentration. This in turn suggests that the dissociation rate constant is much increased compared to that determined for the tight-binding rho-PBP (7 s^{-1}).[9] Because the fluorescence change is likely to depend on the closing of the cleft, an equilibrium constant favoring cleft closure must be maintained. This may in turn limit the extent of weakening P_i binding by mutation, while keeping a fluorescence change.

Table 4 shows a measure of the relative fluorescence of various TMR adducts, including 6-IATR in different solvents, as its adduct with a small molecule, MESNA, and covalently attached to the tight-binding, as well as weak-binding P_i sensor. The relative fluorescence efficiency was determined using the ratio of fluorescence emission to absorbance, each at its maximum wavelength. By this measure, the fluorescence of TMR in aqueous solution is less than half that in ethanol. In both the weak- and the tight-binding variant of rho-PBP, TMR has relatively low fluorescence, even when P_i is bound. There is only a relatively small difference in this fluorescence ratio of rho-PBP in presence and absence of P_i, which is qualitatively in line with the expected mechanism for the fluorescence increase. On binding P_i the TMR labels become at least partially unstacked, leading to an increase in absorbance of the rhodamines. This, in turn, is accompanied by an increase at the fluorescence excitation maximum. The observed fluorescence intensity change on binding P_i is a combination of the increase in extinction coefficient at the exciting wavelength and an increase in fluorescence per unit of absorbance. However, the absorbance spectra are complex with discrete maxima at 516 and 556 nm with the latter peak showing a shoulder in the presence of P_i. The predicted structure, based on molecular modeling, suggests that the two rhodamines in the apo PBP are not exactly parallel, so the stacking is imperfect,[21] at least compared with the situation where rhodamines are freely mobile in solution,[36] and the relative size of the two rhodamine peaks suggests incomplete unstacking when P_i binds. In contrast, monomeric TMR in free solution has the 555 nm peak larger than the 515 nm one. These factors suggest that the stacking/unstacking between the two conformations of rho-PBP is more complex than seen in free solution.

The I76G variant of rho-PBP, rho-PBPw, extends the useable range of the biosensor so P_i can be readily measured in the tens of micromolar range, using substoichiometric protein. The fluorescence response to P_i was ionic strength and pH dependent with the maximum response of 9-fold. While the affinity of rho-PBPw was little affected by pH, there was a decrease with salt concentration (Table 2). These findings highlight the requirement to obtain a calibration for each experimental condition in any assay based on fluorescence. Importantly, the additional, weakening mutation did not affect specificity: none of the molecules tested resulting in a significant fluorescence response (Table 3).

Both previous, high-affinity sensors based on the PBP scaffold have been used in a range of *in vitro* studies.[10,13,34,35,37] The ability of rho-PBPw to be used to detect P_i in a steady-state assay in real time was demonstrated in a test system. The ATPase activity of the helicase, PcrA, showed comparable results using rho-PBPw to those using rho-PBP under the same solution conditions.[35]

The new biosensor has several properties differentiating it from the existing MDCC-PBP and tight-binding rho-PBP. Rhodamines are much more photostable than diethylaminocoumarin, an important property for assays relying on high intensity excitation, such as single molecule and high-throughput studies. High-throughput assays, in particular, also benefit from the extended useable range in two ways. First, the lower affinity allows for the sensor to be used at substoichiometric concentrations relative to P_i, making it more economical, whereas the tight-binding biosensors must be present in significant excess over the highest concentration of P_i. Second, the higher P_i detection range allows reactions to be measured over a longer time span, extending the assay range, for which the sensor can be used. The tight-binding MDCC-PBP and rho-PBP remain particularly suited for rapid reactions, such as single-turnover measurements of P_i release, where sensitivity and rapid response are essential. Importantly, the substoichiometric use and weaker affinity mean that rho-PBPw is likely to be little affected by typical levels P_i contamination that can be present in many biological solutions, buffers, and so forth.[17] In contrast, the tight-binding version binds contaminant P_i stoichiometrically under most assay conditions, so that a significant proportion of the biosensor can be P_i-bound at the start of the assay, increasing the background fluorescence and also decreasing the biosensor free to detect P_i formation.

The development of this biosensor, based on the phosphate binding protein, illustrates the variety of mutational approaches that might be used to achieve the desired weakened binding, while maintaining a useful signal change. The strategy that succeeded was addition of a third glycine in the hinge region to increase its flexibility. In doing so, it widens the range of applications for this type of biosensor.

AUTHOR INFORMATION

Corresponding Author

*E-mail: martin.webb@crick.ac.uk.

Funding

This work was supported by the Francis Crick Institute, which receives its core funding principally from Cancer Research UK, the UK Medical Research Council and the Wellcome Trust.

DOI: 10.1021/acs.biochem.5b00449
Biochemistry 2015, 54, 5054−5062

Notes

The expressionplasmid containing the (A17C, I76G, A197C)PBP gene is available to academic laboratories on request.

The authors declare the following competing financial interest(s): Part of this work is subject of a UK patent application (1505256.6).

■ ACKNOWLEDGMENTS

We thank Steven Howell (The Francis Crick Institute, London) for obtaining mass spectra, Dr. Stephen Martin (The Francis Crick Institute, London) for obtaining CD spectra, and Gordon Reid (The Francis Crick Institute, London) for preparing highly purified nucleotides.

■ ABBREVIATIONS

6-IATR, 6-iodoacetamidotetramethylrhodamine; DTT, dithiothreitol; MEG, 7-methylguanosine; MESNA, 2-mercaptoethanesulfonate; MDCC, *N*-[2-(1-maleimidyl)ethyl]-7-(diethylamino)coumarin-3-carboxamide; MDCC-PBP, (A197C)PBP, labeled with MDCC; PBP, phosphate binding protein; rho-PBP, (A17C,A197C)PBP, labeled with 6-IATR; rho-PBPw, (A17C,I76G,A197C), labeled with 6-IATR; PNPase, purine nucleoside phosphorylase; TMR, tertramethylrhodamine

■ REFERENCES

(1) Bell, R. D., and Doisy, E. A. (1920) Rapid colorimetric methods for the determination of phosphorus in urine and blood. *J. Biol. Chem. 44*, 55−67.

(2) Briggs, A. P. (1922) A modification of the Bell-Doisy phosphate method. *J. Biol. Chem. 53*, 13−16.

(3) Fiske, C. H., and SubbaRow, Y. (1925) The colorimetric determination of phosphorus. *J. Biol. Chem. 66*, 375−400.

(4) Banik, U., and Roy, S. (1990) A continuous fluorimetric assay for ATPase activity. *Biochem. J. 266*, 611−614.

(5) Webb, M. R. (1992) A continuous spectrophotometric assay for inorganic phosphate and for measuring phosphate release kinetics in biological systems. *Proc. Natl. Acad. Sci. U. S. A. 89*, 4884−4887.

(6) Vazquez, M. J., Rodriguez, B., Zapatero, C., and Tew, D. G. (2003) Determination of phosphate in nanomolar range by an enzyme-coupling fluorescent method. *Anal. Biochem. 320* (2), 292−298.

(7) Kunzelmann, S., Solscheid, C., and Webb, M. R. (2014) Fluorescent biosensors: design and application to motility proteins. In *Fluorescent Methods Applied to Molecular Motors, Experientia Supplementum* (Toseland, C. P., and Fili, N., Eds.), Vol. *105*, pp 25−47, Springer, Basel.

(8) Brune, M., Hunter, J. L., Corrie, J. E. T., and Webb, M. R. (1994) Direct, real-time measurement of rapid inorganic phosphate release using a novel fluorescent probe and its application to actomyosin subfragment 1 ATPase. *Biochemistry 33*, 8262−8271.

(9) Okoh, M. P., Hunter, J. L., Corrie, J. E. T., and Webb, M. R. (2006) A biosensor for inorganic phosphate using a rhodamine-labeled phosphate binding protein. *Biochemistry 45*, 14764−14771.

(10) White, H. D., Belknap, B., and Webb, M. R. (1997) Kinetics of nucleoside triphosphate cleavage and phosphate release steps by associated rabbit skeletal actomyosin, measured using a novel fluorescent probe for phosphate. *Biochemistry 36*, 11828−11836.

(11) Webb, M. R. (2007) Development of fluorescent biosensors for probing the function of motor proteins. *Mol. BioSyst. 3*, 249−256.

(12) Gilbert, S. P., Webb, M. R., Brune, M., and Johnson, K. A. (1995) Pathway of processive ATP hydrolysis by kinesin. *Nature 373*, 671−676.

(13) He, Z.-H., Chillingworth, R. K., Brune, M., Corrie, J. E. T., Webb, M. R., and Ferenczi, M. A. (1999) The efficiency of contraction in rabbit skeletal muscle fibres, determined from the rate of release of inorganic phosphate. *J. Physiol. 517*, 839−854.

(14) Hanes, J. W., and Johnson, K. A. (2008) Real-time measurement of pyrophosphate release kinetics. *Anal. Biochem. 372* (1), 125−127.

(15) Salins, L. L. E., Deo, S. K., and Daunert, S. (2004) Phosphate binding protein as the biorecognition element in a biosensor for phosphate. *Sens. Actuators, B 97* (1), 81−89.

(16) Nixon, A. E., Hunter, J. L., Bonifacio, G., Eccleston, J. F., and Webb, M. R. (1998) Purine nucleoside phosphorylase: its use in a spectroscopic assay for inorganic phosphate and to remove inorganic phosphate with the aid of phosphodeoxyribomutase. *Anal. Biochem. 265*, 299−307.

(17) Webb, M. R. (2003) A fluorescent sensor to assay inorganic phosphate. In *Kinetic Analysis of Macromolecules: a Practical Approach* (Johnson, K. A., Ed.), pp 131−152, Oxford University Press, Oxford, U.K.

(18) Luecke, H., and Quiocho, F. A. (1990) High specificity of a phosphate transport protein determined by hydrogen bonds. *Nature 347*, 402−406.

(19) Ledvina, P. S., Yao, N., Choudhary, A., and Quiocho, F. A. (1996) Negative electrostatic surface potential of protein sites specific for anionic ligands. *Proc. Natl. Acad. Sci. U. S. A. 93*, 6786−6791.

(20) Brune, M., Hunter, J. L., Howell, S. A., Martin, S. R., Hazlett, T. L., Corrie, J. E. T., and Webb, M. R. (1998) Mechanism of inorganic phosphate interaction with phosphate binding protein from *Escherichia coli*. *Biochemistry 37*, 10370−10380.

(21) Goncalves, M. B., Dreyer, J., Lupieri, P., Barrera-Patino, P. C., Ippoliti, E., Webb, M. R., Corrie, J. E. T., and Carloni, P. (2013) Structural prediction of a rhodamine-based biosensor and comparison with biophysical data. *Phys. Chem. Chem. Phys. 15*, 2177−2183.

(22) Bird, L. E., Brannigan, J. A., Subramanya, H. S., and Wigley, D. B. (1998) Characterisation of *Bacillus stearothermophilus* PcrA helicase: evidence against an active rolling mechanism. *Nucleic Acids Res. 26*, 2686−2693.

(23) Slatter, A. F., Thomas, C. D., and Webb, M. R. (2009) PcrA helicase tightly couples ATP hydrolysis to unwinding double-stranded DNA, modulated by the replication initiator protein, RepD. *Biochemistry 48*, 6326−6334.

(24) Corrie, J. E. T., and Craik, J. S. (1994) Synthesis and characterisation of pure isomers of iodoacetamidotetramethylrhodamine. *J. Chem. Soc., Perkin Trans. 1*, 2967−2973.

(25) Munasinghe, V. R. N., and Corrie, J. E. T. (2006) Optimised synthesis of 6-iodoacetamidotetramethylrhodamine. *ARKIVOC 2006*, 143−149.

(26) Morita, T., Amemura, M., Makino, K., Shinagawa, H., Magota, K., Otsuji, N., and Nakata, A. (1983) Hyperproduction of phosphate-binding protein, phoS, and pre-phoS proteins in *Escherichia coli* carrying a cloned phoS gene. *Eur. J. Biochem. 130*, 427−435.

(27) Leatherbarrow, R. J. (2009) *GraFit*, version 7, Erithacus Software Ltd, Horley, U.K.

(28) Hirshberg, M., Henrick, K., Haire, L. L., Vasisht, N., Brune, M., Corrie, J. E. T., and Webb, M. R. (1998) The crystal structure of phosphate binding protein labeled with a coumarin fluorophore, a probe for inorganic phosphate. *Biochemistry 37*, 10381−10385.

(29) Gu, H., Lalonde, S., Okumoto, S., Looger, L. L., Scharff-Poulsen, A. M., Grossman, A. R., Kossmann, J., Jakobsen, I., and Frommer, W. B. (2006) A novel analytical method for in vivo phosphate tracking. *FEBS Lett. 580* (25), 5885−5893.

(30) Marvin, J. S., and Hellinga, H. W. (2001) Manipulation of ligand binding affinity by exploitation of conformational coupling. *Nat. Struct. Biol. 8* (9), 795−798.

(31) Millet, O., Hudson, R. P., and Kay, L. E. (2003) The energetic cost of domain reorientation in maltose-binding protein as studied by NMR and fluorescence spectroscopy. *Proc. Natl. Acad. Sci. U. S. A. 100* (22), 12700−12705.

(32) Dwyer, M. A., and Hellinga, H. W. (2004) Periplasmic binding proteins: a versatile superfamily for protein engineering. *Curr. Opin. Struct. Biol. 14* (4), 495−504.

DOI: 10.1021/acs.biochem.5b00449
Biochemistry 2015, 54, 5054−5062

(33) Chambers, R. W., Kajiwara, T., and Kearns, D. R. (1974) Effect of dimer formation on the electronic absorption and emission spectra of ionic dyes. *J. Phys. Chem. 78*, 380−387.
(34) Dillingham, M. S., Wigley, D. B., and Webb, M. R. (2000) Demonstration of unidirectional single-stranded DNA translocation by PcrA helicase: measurement of step size and translocation speed. *Biochemistry 39*, 205−212.
(35) Toseland, C. P., Martinez-Senac, M. M., Slatter, A. F., and Webb, M. R. (2009) The ATPase cycle of PcrA helicase and its coupling to translocation on DNA. *J. Mol. Biol. 392*, 1020−1032.
(36) Ilich, P., Mishra, P. K., Macura, S., and Burghardt, T. P. (1996) Direct observation of rhodamine dimer structures in water. *Spectrochim. Acta, Part A 52* (10), 1323−1330.
(37) Ansell, K. H., Jones, H. M., Whalley, D., Hearn, A., Taylor, D. L., Patin, E. C., Chapman, T. M., Osborne, S. A., Wallace, C., Birchall, K., Large, J., Bouloc, N., Smiljanic-Hurley, E., Clough, B., Moon, R. W., Green, J. L., and Holder, A. A. (2014) Biochemical and antiparasitic properties of inhibitors of the Plasmodium falciparum calcium-dependent protein kinase PfCDPK1. *Antimicrob. Agents Chemother. 58* (10), 6032−6043.
(38) Kunzelmann, S., and Webb, M. R. (2009) A biosensor for fluorescent determination of ADP with high time resolution. *J. Biol. Chem. 284*, 33130−33138.

DOI: 10.1021/acs.biochem.5b00449
Biochemistry 2015, 54, 5054−5062